

NATIONAL INSTITUTE FOR FUSION SCIENCE

Effects of Impurities Released from High Z Test Limiter on Plasma Performance in TEXTOR

Y. Ueda, T. Tanabe, V. Philipps, L. Könen,
A. Pospieszczyk, U. Samm, B. Schweer,
B. Unterberg, M. Wada, N. Hawkes
and N. Noda

(Received - July 8, 1994)

NIFS-293

Aug. 1994

RESEARCH REPORT NIFS Series

This report was prepared as a preprint of work performed as a collaboration research of the National Institute for Fusion Science (NIFS) of Japan. This document is intended for information only and for future publication in a journal after some rearrangements of its contents.

Inquiries about copyright and reproduction should be addressed to the Research Information Center, National Institute for Fusion Science, Nagoya 464-01, Japan.

NAGOYA, JAPAN

Effects of Impurities Released From High Z Test Limiter on Plasma Performance in TEXTOR

Y. Ueda¹, T. Tanabe¹, V. Philipps², L. Könen², A. Pospieszczyk², U. Samm²,
B. Schweer², B. Unterberg², M. Wada³, N. Hawkes⁴, and N. Noda⁵

¹*Faculty of Engineering, Osaka University, 2-1 Yamada-Oka, Suita,
Osaka 565, Japan*

²*Institut für Plasmaphysik, Forschungszentrum Jülich, Ass Euratom -
KFA, 52425 Jülich, Germany*

³*Department of Electronics, Doshisha University, Tsuzukigun, Kyoto
610-03, Japan*

⁴*UKAEA Culham Laboratory, Abingdon, Oxon, UK*

⁵*National Institute for Fusion Science, Furo-cho, Chikusa-ku, Nagoya
464-01, Japan*

A contributed paper orally presented in 11th International Conference on Plasma Surface Interactions in Controlled Fusion Devices held in Mito from May 23 to 27 1994. To be published in Journal of Nuclear Materials.

Abstract

To investigate the feasibility of high Z metals as plasma facing materials, a Mo test limiter was inserted into the TEXTOR edge plasma and the Mo content in the core plasma and its flux from the limiter have been observed.

In OH plasma the additional radiation due to Mo impurities increased with line averaged density \bar{n}_e . Beyond \bar{n}_e of about $3 \times 10^{19} \text{ m}^{-3}$, the central radiation increased strongly with time and a hollow temperature profile appeared. In contrast, Mo impurity radiation decreased with \bar{n}_e in NBI (co-injection) plasma and no clear Mo accumulation in the plasma center was observed. However, when the edge plasma was cooled by neon injection in NBI plasma, the Mo concentration in the plasma center substantially increased.

The Mo flux from the limiter showed no remarkable change during the OH and NBI density scan or with neon cooling. The possible reasons for the Mo behavior in the core plasma are discussed.

[Key Words : TEXTOR, plasma facing materials, High Z materials, molybdenum, tungsten, limiter, impurity behavior, neon cooling]

1. Introduction

Although low Z materials have been mainly considered for plasma facing components (PFCs) of near term devices, high erosion rate and loss of thermal conductivity in carbon based materials have not been completely solved[1]. From these viewpoints, high Z metals (molybdenum and tungsten) are possible candidates for PFCs in the next large tokamak. One of the severe problems of high Z metals is its central accumulation and resultant radiation loss. It is of great importance to find conditions in which this problem can be avoided.

For this study, we inserted movable Mo and W test limiters into the TEXTOR edge plasma and observed high Z impurity release from the limiter and high Z impurity behavior in the core plasma[2, 3]. Since the effects on the plasma performance are similar for Mo- and W-limiters, this paper concentrates on the Mo-limiter results. Mo impurity behaviors are shown under different plasma operation conditions such as OH plasma, NBI plasma and NBI plasma with strong edge cooling by neon injection.

2. Experimental

The experiments have been made under standard TEXTOR operating conditions (deuterium discharge) with a plasma current of 340 kA and a toroidal field of 2.2 T. TEXTOR[4] is a limiter tokamak with a major radius of 175 cm and a minor radius of 46 cm which is determined by ALT-II toroidal belt limiter. Co-injection neutral beam (hydrogen) with a power of 1.25 MW was used in the experiments.

Mo test limiter was inserted from the bottom of the torus up to a minor radius of 43 cm, which is 3 cm deeper into the plasma than the

ALT-II main limiter ($r = 46$ cm). The dimensions of the limiter are the followings; 10 cm long in toroidal direction and 6 cm wide in poloidal direction with a round surface shape of a toroidal radius of 8.5 cm and a poloidal radius of 6.5 cm[5]. Integrated heat load to the test limiter was estimated from temperature rise of the limiter head measured by two thermocouples.

The fluxes of impurities and deuterium were determined by spectral line intensities from neutrals and low charged ions measured tangentially in front of the limiter surface. The impurity behavior in the core plasma was studied by total radiation, VUV lines and soft Xray. The total radiation was measured by an eight channel bolometer array. The radial profile of radiated power $P_{\text{rad}}(r)$ was deduced by an Abel-inversion technique. The VUV lines of MoXXXI(17.7 nm) and MoXXVII(52.7 nm) and the soft Xray emission from L-shell electron (~ 2.5 keV) were used for this study.

The radial profiles of electron temperature and density were measured with an ECE system and an array of interferometers, respectively. Edge electron temperature and density profile were determined using a He beam technique[6].

3. Radiation characteristics of OH and NBI plasmas

Figure 1 shows the radial profiles of the radiated power for OH and NBI plasmas with the test limiter position as a parameter for plasmas with equal \bar{n}_e of $2.5 \times 10^{19} \text{ m}^{-3}$. All data shown in Fig. 1 are taken under stable conditions during current flat top phase ($t = 1.0$ s for OH, $t = 1.6$ s for NBI) except one OH case ($r_{\text{lim}} = 44.0$ cm, 'unstable'), in which the

central radiation rapidly increased and hollow electron temperature profile appeared after $t = 1.0$ s, and finally a minor disruption occurred. More details of this instability are described elsewhere[2].

In OH plasma, the radiation within a plasma radius of about 30 cm increased as the test limiter was inserted. MoXXVII and soft Xray (~ 2.5 keV) radiating in the center in this OH plasma also increased. However, central electron temperature and density showed almost no change (less than 3%) as the limiter was inserted until a limiter position r_{lim} of 44.5 cm. At r_{lim} of 44.0 cm, total radiation P_{rad} increased by about 60%, leading to a reduction of the central electron temperature by about 10%. This condition seems marginal and the plasma showed two different features, such as ‘stable’ and ‘unstable’.

In NBI plasma shown in Fig.1(b), the increment of the radiation was very low compared with the OH plasma even with the limiter at $r_{lim} = 44.0$ cm. An energy ratio E_{lim} / E_{conv} reached about 10% in this case, where E_{lim} denotes total deposition energy onto the limiter and E_{conv} denotes total convective energy calculated by integrating the external heating power subtracted by the total radiation over the discharge duration. The maximum power flux reached about 20 MW/m² for 2 seconds. No clear change of the electron temperature and density (less than 3%) in the core plasma was observed and P_{rad} increased by 20%.

Figure 2 shows the dependence on \bar{n}_e of the increment in the local radiation power ΔP_{rad} at the magnetic axis ($r/a = 0$) and that at the position of $r/a = 0.6$ with a fixed limiter position ($r_{lim} = 44.5$ cm for OH and $r_{lim} = 45.0$ cm for NBI). In OH plasma, as \bar{n}_e was increased from $1.5 \times 10^{19} \text{ m}^{-3}$ to $3.2 \times 10^{19} \text{ m}^{-3}$, ΔP_{rad} in the plasma center rapidly increased. Beyond \bar{n}_e of about $3 \times 10^{19} \text{ m}^{-3}$, the plasma was no longer stable and

ran into minor disruption, as described before.

In contrast to OH plasma, ΔP_{rad} of NBI plasma at $r/a = 0.6$ increased as \bar{n}_e was decreased from $5 \times 10^{19} \text{ m}^{-3}$ to $2 \times 10^{19} \text{ m}^{-3}$. Although the deposition energy to the test limiter did not depend significantly on \bar{n}_e , ΔP_{rad} in high \bar{n}_e was very small. In addition, the central radiation was always low regardless of \bar{n}_e , indicating that some impurity sweeping out mechanism exists in NBI plasma.

4. Neon cooling

In order to reduce the heat load to PFCs, edge plasma cooling is one of the attractive technologies. In TEXTOR, neon injection has been proved to be a promising method for edge cooling without changing the central electron temperature[7]. In our experiment, the ratio of the radiation power P_{rad} to the heating power P_{heat} increased from 0.40 (without neon cooling) to about 0.85. Under this condition, the flux ratio of neon to deuterium measured on the poloidal limiter located at the upper side of the torus of $r = 48 \text{ cm}$ was about 0.12. The deposition energy to the limiter, E_{lim} , with the limiter position of $r_{\text{lim}} = 45 \text{ cm}$ decreased from 120 kJ to 50 kJ with neon cooling, while the electron temperature at $r = 46 \text{ cm}$ also decreased from 35 eV to 15 eV.

Figure 3 shows the evolution of D-flux to the ALT-II limiter and the MoXXXI emission from the central chord of the plasma. The intensity of MoXXXI increased with neon injection by a factor of about 4, though D-flux to ALT-II was reduced. In contrast, the low Z impurity content (carbon and oxygen) did not change significantly. The MoXXXI emission comes from the plasma central region (central electron temperature is about 1.3 keV), indicating that central Mo concentration increased

strongly.

Figure 4 shows the flux of D, C and Mo from the Mo test limiter as a function of the flux ratio of Ne/D. Although the D-flux shows appreciable reduction with increase of the flux ratio of Ne/D, the Mo- and C-fluxes are nearly independent of the flux ratio (Mo-flux increases by only 10-20%). Obviously the decrease of the sputtered Mo by C due to the decrease of edge electron temperature was roughly compensated by the sputtering of Mo by Ne. However, this small change of the Mo-flux with neon cooling is not enough to account for the considerable increase in the central Mo concentration. According to Samm et al.[8], the particle confinement time of helium is increased with neon cooling. Therefore, Mo particle confinement might increase and cause the increase of Mo concentration with neon cooling. But more detailed studies are necessary.

5. Discussion

In this discussion, we will discuss the relation between Mo behavior in the plasma and that in front of the limiter. The local electron temperature and density did not show clear change by inserting the limiter. Meanwhile, the low Z impurity generation from ALT-II limiter was unchanged by the insertion of test limiter, since most of the convective energy loss E_{conv} flowed into the ALT-II limiter (more than 96% at $r_{\text{lim}} = 45$ cm). Therefore, the increment of the radiation ΔP_{rad} can be attributed to an increase of Mo-density. Assuming a steady state coronal model, Mo-density can be estimated from ΔP_{rad} using the cooling rate of Mo given by D. Post et al.[9]. The estimated Mo densities of NBI plasma at $r/a = 0.6$ (Fig.2) are $6.4 \times 10^{15} \text{ m}^{-3}$ for $\bar{n}_e = 2.0 \times 10^{19}$

m^{-3} and $1.6 \times 10^{15} \text{ m}^{-3}$ for $\bar{n}_e = 4.0 \times 10^{19} \text{ m}^{-3}$ corresponding to the concentrations n_{Mo}/n_e of 2.9×10^{-4} and 3.6×10^{-5} , respectively.

In our experimental conditions, Mo atoms were sputtered mainly by low Z impurities (C and O)[2, 3]. With decrease of \bar{n}_e , the electron temperature at the plasma edge and the sputtering yield of Mo increased. However, the change of the absolute Mo-flux with \bar{n}_e was relatively small; the Mo-flux decreased by less than 40% during the OH and NBI density scan (from $\bar{n}_e = 2.0 \times 10^{19} \text{ m}^{-3}$ to $4.0 \times 10^{19} \text{ m}^{-3}$). Therefore, the variation of the total number of Mo in the core plasma (more than a factor of 4) is much larger than that of the Mo-flux from the test limiter. This means that for a better understanding of the Mo behavior the particle confinement in the core plasma and the impurity screening effects in front of the test limiter must be considered.

In OH plasmas, the increase in the Mo content at high \bar{n}_e could be related to an increase in the particle confinement. The impurity confinement time τ_p has earlier been measured in TEXTOR using the laser blow-off method[10]. It was shown that τ_p increases in OH plasmas with \bar{n}_e and grows rapidly in detached plasmas.

In NBI plasma, the significant decrease of the Mo content in high \bar{n}_e could be partly due to a change of the impurity screening effects in front of the test limiter. Figure 5 shows the ionization length of Mo neutral near the limiter surface as a function of \bar{n}_e . As \bar{n}_e was increased, the edge electron density also increased and ionization length decreased. The gyroradius of Mo^+ with an energy of 4 eV is about 1.3 mm. When the ionization length becomes less than this radius ($\bar{n}_e \geq 4 \times 10^{19} \text{ m}^{-3}$, $n_e \geq 1 \times 10^{19} \text{ m}^{-3}$ at $r = 45 \text{ cm}$), the probability of the Mo ion reaching the limiter surface within the first period of gyromotion is very high. This

means that the impurity screening effects could be much stronger at higher \bar{n}_e (higher edge density).

6. Conclusions

In OH plasma, radiation increment ΔP_{rad} by inserting the Mo test limiter increased with increase of \bar{n}_e and beyond \bar{n}_e of about $3 \times 10^{13} \text{ cm}^{-3}$ the minor disruption occurred. In NBI plasma, however, ΔP_{rad} increased with decrease of \bar{n}_e . In addition, central peaked radiation observed in OH plasma was not observed in NBI plasma. The central Mo-density increased significantly with neon injection, though the edge electron temperature and the deposition energy to the limiter were reduced.

The Mo-flux from the test limiter did not change remarkably during the OH and NBI density scan or with neon cooling in contrast to the Mo-density in the core plasma. An increased impurity confinement at high density OH plasma and the impurity screening effects in NBI plasma could be related to these Mo behaviors.

Acknowledgements

One of the authors (Y. Ueda) thanks Dr. S. Goto and Dr. M. Nishikawa in Osaka University (Japan) for their support of this study.

This work was carried out under the collaborating research program at the National Institute for Fusion Science.

References

- [1] T. Tanabe, N. Noda and H. Nakamura, J. Nucl. Mater. **196-198** (1992) 11.
- [2] V. Philipps, et al., Submitted to Nucl. Fusion.
- [3] T. Tanabe, V. Philipps, Y. Ueda, B. Unterberg, A. Pospieszczyk, B. Schweer, P. Wienhold, M. Rubel and B. Emmoth, J. Nucl. Mater. (1994)
- [4] H. Soltwisch, et al., Plasma Phys. Contr. Fusion **26** (1984) 23.
- [5] V. Philipps, U. Samm, M. Z. Tokar, B. Unterberg, A. Pospieszczyk and B. Schweer, Nucl. Fusion **33** (1993) 953.
- [6] B. Schweer, G. Mank, A. Pospieszczyk, B. Brosda and B. Pohlmeier, J. Nucl. Mater. **196-198** (1992) 174.
- [7] U. Samm, et al. in: Proc. 18th Europ. Conf. on Controlled Fusion and Plasma Physics, Berlin, 1991, p. 157.
- [8] U. Samm, et al., J. Nucl. Mater. **196-198** (1992) 633.
- [9] D. E. Post, R. V. Jensen, C. B. Tarter, W. H. Grasberger and W. A. Lokke, At. Data Nucl. Data Tables **20** (1977) 397.
- [10] J. Castracane, Y. Demers, L. Könen and A. Pospieszczyk, Nucl. Fusion **27** (1987) 1921.

Figure Captions

- Fig. 1. Radial profiles of radiated power in OH(a) and in NBI(b) plasmas for different Mo limiter position ($\bar{n}_e = 2.5 \times 10^{13} \text{ cm}^{-3}$).
- Fig. 2. Radiation increment ΔP_{rad} at the positions of the magnetic axis ($r/a = 0$, where a is the minor radius, \square) and at $r/a = 0.6$ (\circ) for OH plasma at $r_{\text{lim}} = 44.5 \text{ cm}$ (a), and for NBI plasma at $r_{\text{lim}} = 45.0 \text{ cm}$ (b).
- Fig. 3. Time evolution of D-flux from the ALT-II main limiter, a VUV line of MoXXXI (17.7 nm), and a NeVIII line for NBI plasma with \bar{n}_e of $3 \times 10^{19} \text{ m}^{-3}$ with neon cooling.
- Fig. 4. D-, Mo- and C-fluxes on the Mo test limiter as a function of flux ratio of Ne/D. The fluxes are integrated in the poloidal direction (unit $\text{cm}^{-1}\text{s}^{-1}$).
- Fig.5 Ionization length of Mo neutral determined by the decay length of MoI light intensity near the test limiter for OH plasma(\bullet) and NBI plasma(\circ). Gyroradius of Mo^+ (4 eV) is about 1.3 mm.

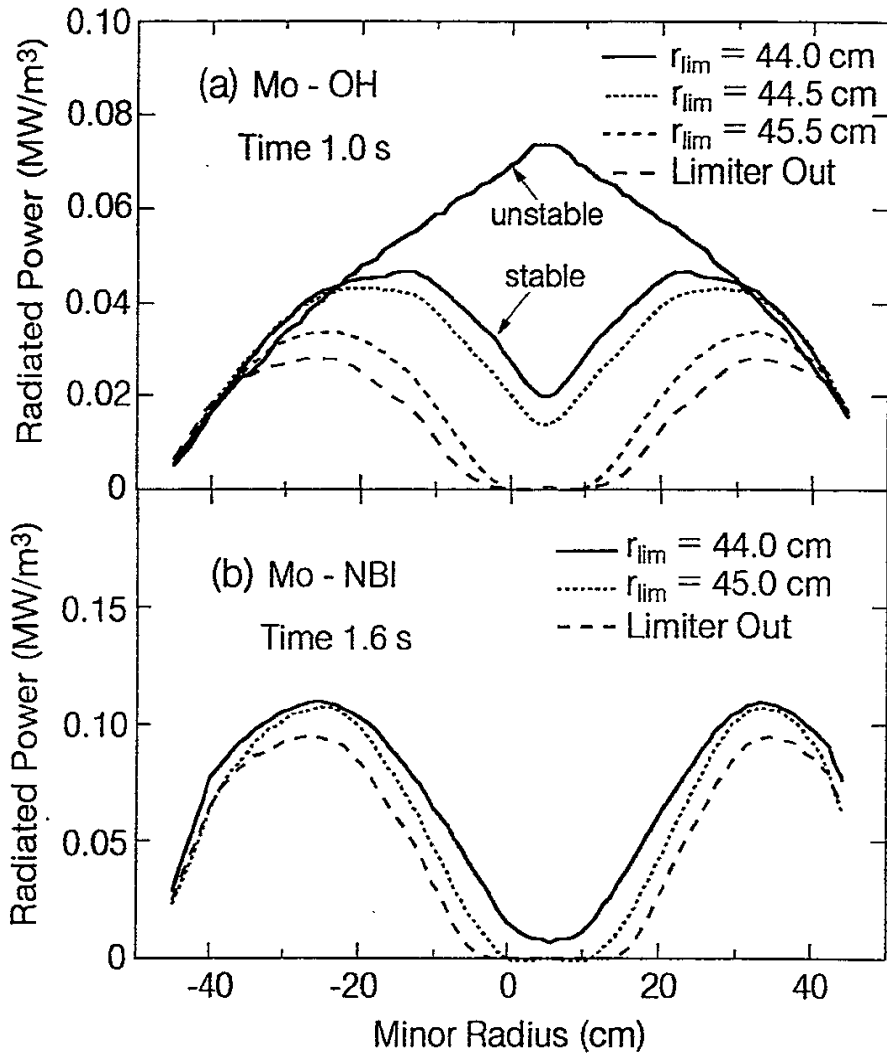


Fig. 1. Radial profiles of radiated power in OH(a) and in NBI(b) plasmas for different Mo limiter position ($\bar{n}_e = 2.5 \times 10^{13} \text{ cm}^{-3}$).

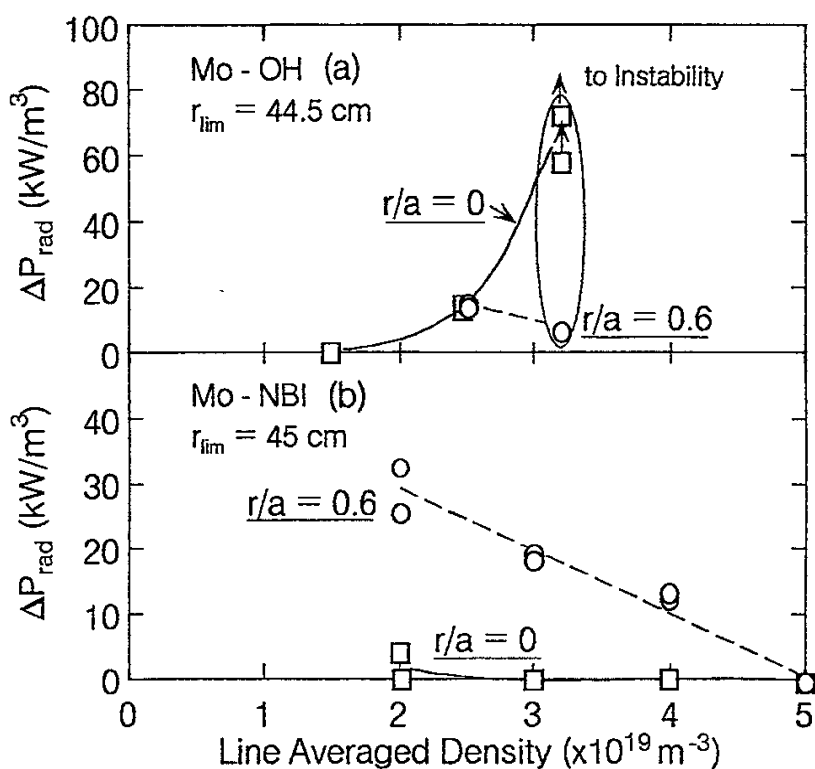


Fig. 2. Radiation increment ΔP_{rad} at the positions of the magnetic axis ($r/a = 0$, where a is the minor radius, \square) and at $r/a = 0.6$ (\circ) for OH plasma at $r_{\text{lim}} = 44.5 \text{ cm}$ (a), and for NBI plasma at $r_{\text{lim}} = 45.0 \text{ cm}$ (b).

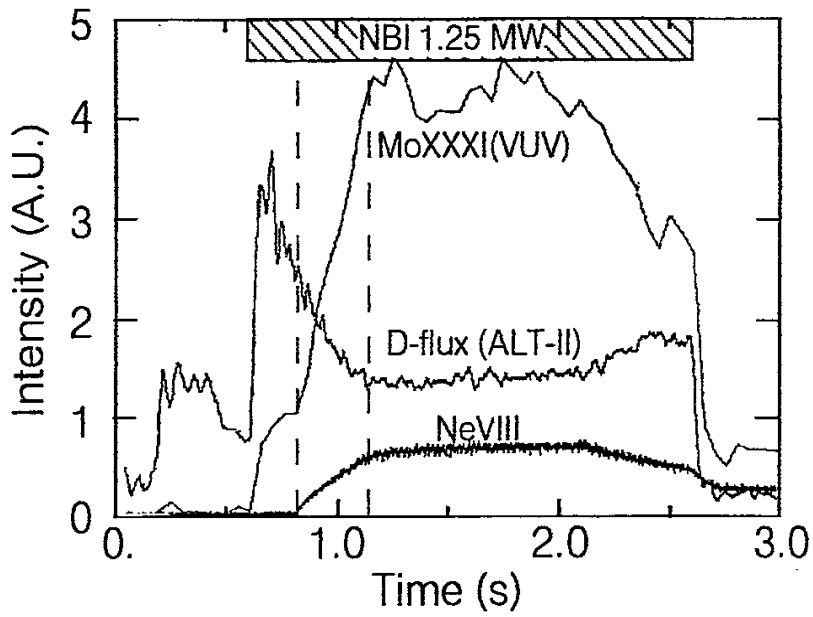


Fig. 3. Time evolution of D-flux from the ALT-II main limiter, a VUV line of MoXXXI (17.7 nm), and a NeVIII line for NBI plasma with \bar{n}_e of $3 \times 10^{19} \text{ m}^{-3}$ with neon cooling.

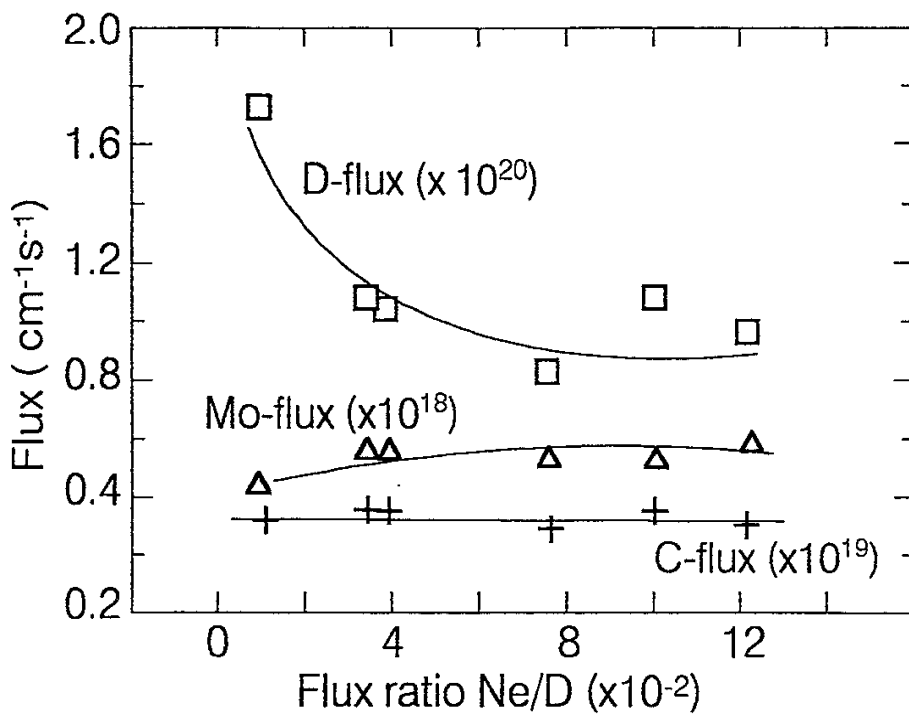


Fig. 4. D-, Mo- and C-fluxes on the Mo test limiter as a function of flux ratio of Ne/D. The fluxes are integrated in the poloidal direction (unit $\text{cm}^{-1}\text{s}^{-1}$).

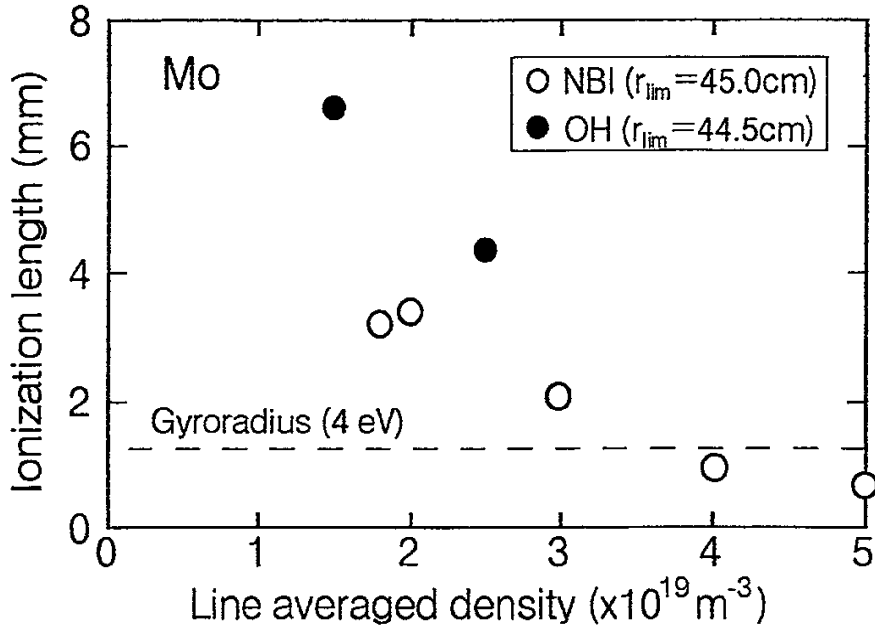


Fig.5 I onization length of Mo neutral determined by the decay length of MoI light intensity near the test limiter for OH plasma(●) and NBI plasma(○). Gyroradius of Mo^+ (4 eV) is about 1.3 mm.

Recent Issues of NIFS Series

- NIFS-250 A. Iiyoshi, H. Momota, O. Motojima, M. Okamoto, S. Sudo, Y. Tomita, S. Yamaguchi, M. Ohnishi, M. Onozuka, C. Uenosono,
Innovative Energy Production in Fusion Reactors; Oct. 1993
- NIFS-251 H. Momota, O. Motojima, M. Okamoto, S. Sudo, Y. Tomita, S. Yamaguchi, A. Iiyoshi, M. Onozuka, M. Ohnishi, C. Uenosono,
Characteristics of D-³He Fueled FRC Reactor: ARTEMIS-L, Nov. 1993
- NIFS-252 Y. Tomita, L.Y. Shu, H. Momota,
Direct Energy Conversion System for D-³He Fusion, Nov. 1993
- NIFS-253 S. Sudo, Y. Tomita, S. Yamaguchi, A. Iiyoshi, H. Momota, O. Motojima, M. Okamoto, M. Ohnishi, M. Onozuka, C. Uenosono,
Hydrogen Production in Fusion Reactors, Nov. 1993
- NIFS-254 S. Yamaguchi, A. Iiyoshi, O. Motojima, M. Okamoto, S. Sudo, M. Ohnishi, M. Onozuka, C. Uenosono,
Direct Energy Conversion of Radiation Energy in Fusion Reactor, Nov. 1993
- NIFS-255 S. Sudo, M. Kanno, H. Kaneko, S. Saka, T. Shirai, T. Baba,
Proposed High Speed Pellet Injection System "HIPEL" for Large Helical Device
Nov. 1993
- NIFS-256 S. Yamada, H. Chikaraishi, S. Tanahashi, T. Mito, K. Takahata, N. Yanagi, M. Sakamoto, A. Nishimura, O. Motojima, J. Yamamoto, Y. Yonenaga, R. Watanabe,
Improvement of a High Current DC Power Supply System for Testing the Large Scaled Superconducting Cables and Magnets; Nov. 1993
- NIFS-257 S. Sasaki, Y. Uesugi, S. Takamura, H. Sanuki, K. Kadota,
Temporal Behavior of the Electron Density Profile During Limiter Biasing in the HYBTOK-II Tokamak; Nov. 1993
- NIFS-258 K. Yamazaki, H. Kaneko, S. Yamaguchi, K.Y. Watanabe, Y. Taniguchi, O. Motojima, LHD Group,
Design of Central Control System for Large Helical Device (LHD); Nov. 1993
- NIFS-259 S. Yamada, T. Mito, A. Nishimura, K. Takahata, S. Satoh, J. Yamamoto, H. Yamamura, K. Masuda, S. Kashiwara, K. Fukusada, E. Tada,
Reduction of Hydrocarbon Impurities in 200L/H Helium Liquefier-Refrigerator System; Nov. 1993
- NIFS-260 B.V. Kuteev,

Pellet Ablation in Large Helical Device; Nov. 1993

- NIFS-261 K. Yamazaki,
Proposal of "MODULAR HELIOTRON": Advanced Modular Helical System Compatible with Closed Helical Divertor; Nov. 1993
- NIFS-262 V.D.Pustovitov,
Some Theoretical Problems of Magnetic Diagnostics in Tokamaks and Stellarators; Dec. 1993
- NIFS-263 A. Fujisawa, H. Iguchi, Y. Hamada
A Study of Non-Ideal Focus Properties of 30° Parallel Plate Energy Analyzers; Dec. 1993
- NIFS-264 K. Masai,
Nonequilibria in Thermal Emission from Supernova Remnants; Dec. 1993
- NIFS-265 K. Masai, K. Nomoto,
X-Ray Enhancement of SN 1987A Due to Interaction with its Ring-like Nebula; Dec. 1993
- NIFS-266 J. Uramoto
A Research of Possibility for Negative Muon Production by a Low Energy Electron Beam Accompanying Ion Beam; Dec. 1993
- NIFS-267 H. Iguchi, K. Ida, H. Yamada, K. Itoh, S.-I. Itoh, K. Matsuoka, S. Okamura, H. Sanuki, I. Yamada, H. Takenaga, K. Uchino, K. Muraoka,
The Effect of Magnetic Field Configuration on Particle Pinch Velocity in Compact Helical System (CHS); Jan. 1994
- NIFS-268 T. Shikama, C. Namba, M. Kosuda, Y. Maeda,
Development of High Time-Resolution Laser Flash Equipment for Thermal Diffusivity Measurements Using Miniature-Size Specimens; Jan. 1994
- NIFS-269 T. Hayashi, T. Sato, P. Merkel, J. Nührenberg, U. Schwenn,
Formation and 'Self-Healing' of Magnetic Islands in Finite- β Helias Equilibria; Jan. 1994
- NIFS-270 S. Murakami, M. Okamoto, N. Nakajima, T. Mutoh,
Efficiencies of the ICRF Minority Heating in the CHS and LHD Plasmas; Jan. 1994
- NIFS-271 Y. Nejoh, H. Sanuki,
Large Amplitude Langmuir and Ion-Acoustic Waves in a Relativistic Two-Fluid Plasma; Feb. 1994

- NIFS-272 A. Fujisawa, H. Iguchi, A. Taniike, M. Sasao, Y. Hamada,
A 6MeV Heavy Ion Beam Probe for the Large Helical Device;
Feb. 1994
- NIFS-273 Y. Hamada, A. Nishizawa, Y. Kawasumi, K. Narihara, K. Sato, T. Seki,
K. Toi, H. Iguchi, A. Fujisawa, K. Adachi, A. Ejiri, S. Hidekuma,
S. Hirokura, K. Ida, J. Koong, K. Kawahata, M. Kojima, R. Kumazawa,
H. Kuramoto, R. Liang, H. Sakakita, M. Sasao, K. N. Sato, T. Tsuzuki,
J. Xu, I. Yamada, T. Watari, I. Negi,
*Measurement of Profiles of the Space Potential in JIPP T-IIU
Tokamak Plasmas by Slow Poloidal and Fast Toroidal Sweeps of a
Heavy Ion Beam;* Feb. 1994
- NIFS-274 M. Tanaka,
A Mechanism of Collisionless Magnetic Reconnection; Mar. 1994
- NIFS-275 A. Fukuyama, K. Itoh, S.-I. Itoh, M. Yagi and M. Azumi,
Isotope Effect on Confinement in DT Plasmas; Mar. 1994
- NIFS-276 R.V. Reddy, K. Watanabe, T. Sato and T.H. Watanabe,
*Impulsive Alfvén Coupling between the Magnetosphere and
Ionosphere;* Apr. 1994
- NIFS-277 J. Uramoto,
*A Possibility of π^- Meson Production by a Low Energy Electron
Bunch and Positive Ion Bunch;* Apr. 1994
- NIFS-278 K. Itoh, S.-I. Itoh, A. Fukuyama, M. Yagi and M. Azumi,
*Self-sustained Turbulence and L-mode Confinement in Toroidal
Plasmas II;* Apr. 1994
- NIFS-279 K. Yamazaki and K.Y. Watanabe,
*New Modular Heliotron System Compatible with Closed Helical
Divertor and Good Plasma Confinement;* Apr. 1994
- NIFS-280 S. Okamura, K. Matsuoka, K. Nishimura, K. Tsumori, R. Akiyama,
S. Sakakibara, H. Yamada, S. Morita, T. Morisaki, N. Nakajima,
K. Tanaka, J. Xu, K. Ida, H. Iguchi, A. Lazaros, T. Ozaki, H. Arimoto,
A. Ejiri, M. Fujiwara, H. Idei, O. Kaneko, K. Kawahata, T. Kawamoto,
A. Komori, S. Kubo, O. Motojima, V.D. Pustovitov, C. Takahashi, K. Toi
and I. Yamada,
High-Beta Discharges with Neutral Beam Injection in CHS,
Apr; 1994
- NIFS-281 K. Kamada, H. Kinoshita and H. Takahashi,
*Anomalous Heat Evolution of Deuteron Implanted Al on Electron
Bombardment ;* May 1994
- NIFS-282 H. Takamaru, T. Sato, K. Watanabe and R. Horiuchi,

Super Ion Acoustic Double Layer; May 1994

- NIFS-283 O.Mitarai and S. Sudo
Ignition Characteristics in D-T Helical Reactors; June 1994
- NIFS-284 R. Horiuchi and T. Sato,
Particle Simulation Study of Driven Magnetic Reconnection in a Collisionless Plasma; June 1994
- NIFS-285 K.Y. Watanabe, N. Nakajima, M. Okamoto, K. Yamazaki, Y. Nakamura, M. Wakatani,
Effect of Collisionality and Radial Electric Field on Bootstrap Current in LHD (Large Helical Device); June 1994
- NIFS-286 H. Sanuki, K. Itoh, J. Todoroki, K. Ida, H. Idei, H. Iguchi and H. Yamada,
Theoretical and Experimental Studies on Electric Field and Confinement in Helical Systems; June 1994
- NIFS-287 K. Itoh and S.-I. Itoh,
Influence of the Wall Material on the H-mode Performance; June 1994
- NIFS-288 K. Itoh, A. Fukuyama, S.-I. Itoh, M. Yagi and M. Azumi
Self-Sustained Magnetic Braiding in Toroidal Plasmas July 1994
- NIFS-289 Y. Nejoh,
Relativistic Effects on Large Amplitude Nonlinear Langmuir Waves in a Two-Fluid Plasma; July 1994
- NIFS-290 N. Ohyabu, A. Komori, K. Akaishi, N. Inoue, Y. Kubota, A.I. Livshit, N. Noda, A. Sagara, H. Suzuki, T. Watanabe, O. Motojima, M. Fujiwara, A. Iiyoshi,
Innovative Divertor Concepts for LHD; July 1994
- NIFS-291 H. Idei, K. Ida, H. Sanuki, S. Kubo, H. Yamada, H. Iguchi, S. Morita, S. Okamura, R. Akiyama, H. Arimoto, K. Matsuoka, K. Nishimura, K. Ohkubo, C. Takahashi, Y. Takita, K. Toi, K. Tsumori and I. Yamada,
Formation of Positive Radial Electric Field by Electron Cyclotron Heating in Compact Helical System; July 1994
- NIFS-292 N. Noda, A. Sagara, H. Yamada, Y. Kubota, N. Inoue, K. Akaishi, O. Motojima, K. Iwamoto, M. Hashiba, I. Fujita, T. Hino, T. Yamashina, K. Okazaki, J. Rice, M. Yamage, H. Toyoda and H. Sugai,
Boronization Study for Application to Large Helical Device; July 1994